Control of Actin and Calcium for Chitin Synthase Delivery to the Hyphal Tip of *Aspergillus*

Norio Takeshita

Contents

1 Introduction 114
2 Chitin Biosynthesis 114
3 Transport of Chitin Synthase 116
4 Super-resolution Imaging and Cluster Analysis of Chitin Synthase 118
5 Pulse-Chase Analysis of mEosFP-ChsB After Photoconversion 119
6 Oscillation of Fungal Tip Growth 121
7 Ca^{2+} Oscillation 122
8 Biological Meaning of Oscillations 123
9 Conclusion and Perspective 124
References 125

Abstract Filamentous fungi are covered by a cell wall consisting mainly of chitin and glucan. The synthesis of chitin, a β-1,4-linked homopolymer of *N*-acetylglucosamine, is essential for hyphal morphogenesis. Fungal chitin synthases are integral membrane proteins that have been classified into seven classes. ChsB, a class III chitin synthase, is known to play a key role in hyphal tip growth and has been used here as a model to understand the cell biology of cell wall biosynthesis in *Aspergillus nidulans*. Chitin synthases are transported on secretory vesicles to the plasma membrane for new cell wall synthesis. Super-resolution localization imaging as a powerful biophysical approach indicated dynamics of the Spitzenkörper where spatiotemporally regulated exocytosis and cell extension, whereas high-speed pulse-chase imaging has revealed ChsB transport mechanism mediated by kinesin-1 and myosin-5. In addition, live imaging analysis showed correlations among intracellular Ca^{2+} levels, actin assembly, and exocytosis in

N. Takeshita (✉)
Microbiology Research Center for Sustainability (MiCS), Faculty of Life and Environmental Sciences, University of Tsukuba, Tsukuba, Japan
e-mail: takeshita.norio.gf@u.tsukuba.ac.jp

Current Topics in Microbiology and Immunology (2020) 425: 113–129
https://doi.org/10.1007/82_2019_193

Published Online: 24 January 2020

growing hyphal tips. This suggests that pulsed Ca^{2+} influxes coordinate the temporal control of actin assembly and exocytosis, which results in stepwise cell extension. It is getting clear that turgor pressure and cell wall pressure are involved in the activation of Ca^{2+} channels for Ca^{2+} oscillation and cell extension. Here the cell wall synthesis and tip growth meet again.

1 Introduction

Filamentous fungi grow as highly polarized tubular cells called hyphae that extend the cell body at one end in a process called 'tip growth.' Cell extension sites are maintained at hyphal tips, where simultaneous actin assembly, exocytosis, and tip extension occur (Fischer et al. 2008; Riquelme et al. 2011; Takeshita et al. 2014; Riquelme et al. 2018). Several filamentous fungi that extend cells in this manner are excellent systems for analyzing this process (Lopez-Franco et al. 1994). Some filamentous fungi are pathogenic to animals and plants and invade host cells via hyphal growth (Perez-Nadales et al. 2014). Others have uses in biotechnology and food production such as enzyme production and fermentation, respectively, as they secrete large amounts of enzymes (Kobayashi et al. 2007; Punt et al. 2002). Both the pathogenicity and enzyme secretory ability of fungi are closely associated with hyphal growth. Thus, understanding polarized growth in filamentous fungi can provide insights that are important to medicine, agriculture, and biotechnology.

2 Chitin Biosynthesis

The cell wall not only imparts physical strength to the cell but also plays a role in transmitting information about the natural or artificial environmental conditions to the inside of the cell. The cell walls of *Aspergillus fumigatus* are composed of β-(1,3)-glucan, chitin, β-(1,3)-/β-(1,4)-glucan, ∝-(1,3)-glucan, galactomannan (GM), galactosaminogalactan (GAG), and proteins (Latge et al. 2017). Most cell wall proteins are modified by *N*-glycan, *O*-glycan, and/or a glycosylphosphatidylinositol anchor. These components are complexly intertwined to form the three-dimensional structure of cell walls (Fig. 1a). During hyphal tip growth, various glycan synthases, including β-(1,3)-glucan synthases, chitin synthases, and ∝-(1,3)-glucan synthases, are transported to the tips by secretory vesicles. The transported glycan synthases generate the corresponding glycans, which then penetrate into the interstices of the cell wall skeleton, where they act like cement. Thus, the hyphae grow by forming a complicated three-dimensional structure.

Chitin, a β-(1,4)-linked polymer of *N*-acetylglucosamine (GlcNAc), is a major skeletal component of the cell wall of *A. fumigatus* and gives the wall mechanical rigidity. The higher amount of chitin (>10%) present in the walls of *Aspergillus* sp. as compared to yeast (Blumenthal and Roseman 1957; Johnston 1965) indicates

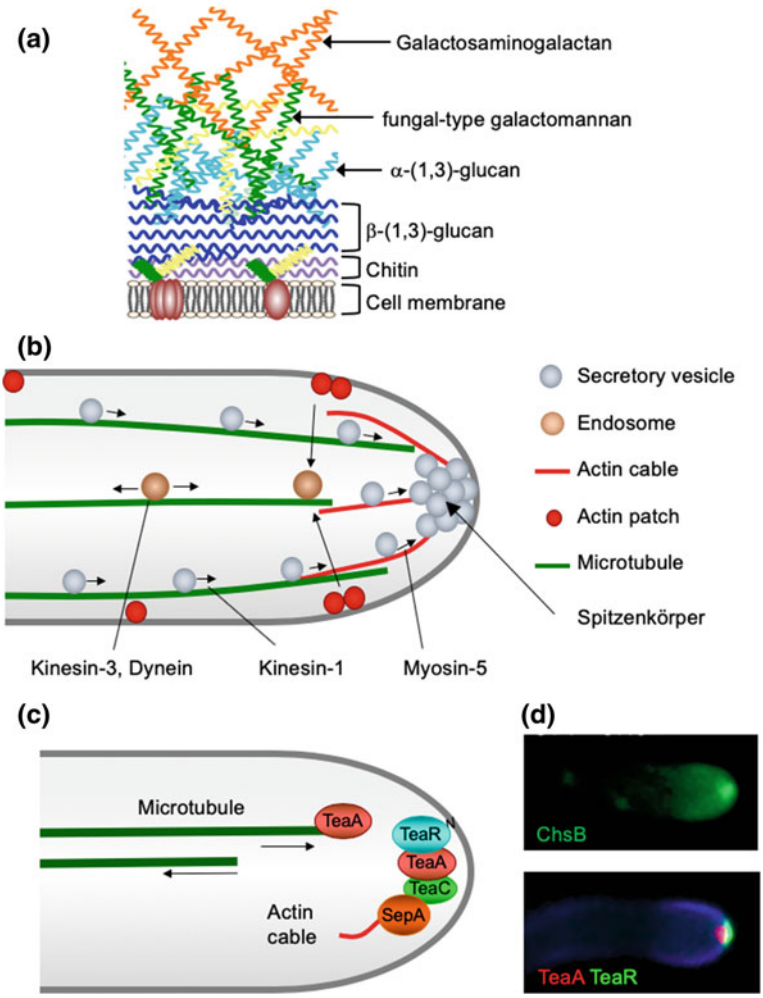

Fig. 1 Scheme of tip growth in *A. nidulans* hyphae. **a** Schematic representation of structural organization of the cell surface of *Aspergillus.* The different polysaccharides have their roles; glucans are the most abundant compounds in the fungal cell walls and an amorphous gel-like matrix, chitin as a cell wall skeleton. **b** Secretory vesicle trafficking via the microtubule and actin cytoskeleton depending on kinesin-1 and myosin-5, respectively. Before fusion with the plasma membrane, secretion vesicles accumulate at Spitzenkörper. **c** Scheme of the function of cell end markers in *A. nidulans*. **d** Localization of GFP-ChsB at Spitzenkörper (upper). Localization of cell end markers mRFP1-TeaA and GFP-TeaR at the hyphal tip (lower)

that the synthesis of chitin is essential for hyphal morphogenesis (Rogg et al. 2012). Chitin is biosynthesized by several chitin synthases localized at the plasma membrane; these are responsible for the sequential synthesis of GlcNAc using UDP-GlcNAc as a sugar donor.

Fungal chitin synthases are integral membrane proteins that have been classified into seven classes and three divisions according to their structural properties (Lenardon et al. 2010a, b; Gonçalves et al. 2016). *Aspergillus fumigatus* and *Aspergillus nidulans* have eight different chitin synthases (ChsA-ChsD, ChsF, ChsG, CsmA, and CmsB in *A. nidulans*) (Horiuchi 2009; de Groot et al. 2009). Among these, ChsB, a class III chitin synthase, is known to play a key role in hyphal tip growth, maintenance of cell wall integrity, and development (Yanai et al. 1994; Borgia et al. 1996; Fukuda et al. 2009). The *chsB* disruptant hyphae have enlarged tips, a high degree of branching, and disorganized lateral walls (Borgia et al. 1996). Class III chitin synthases are important for hyphal morphology, cell wall integrity, and pathogenicity in other filamentous fungi as well (Rogg et al. 2012; Muszkieta et al. 2014). Meanwhile, ChsA and ChsC are required for the formation of the septum and a normal conidiophore (Motoyama et al. 1994; Fujiwara et al. 2000; Ichinomiya et al. 2005). CsmA and CsmB, that are widely distributed in filamentous fungi and dimorphic yeasts but lacking in *S. cerevisiae* and *S. pombe,* have myosin motor-like domains (Fujiwara et al. 1997). The myosin motor-like domains bind to actin filaments, suggesting a direct link between the actin cytoskeleton and polarized cell wall synthesis (Takeshita et al. 2005, 2006). ChsB has been used as a model to understand the vesicles trafficking in chitin synthesis.

3 Transport of Chitin Synthase

Polarized growth of fungal hyphae is sustained by the continuous delivery of vesicles loaded with biomolecules to the hyphal tips (Rittenour et al. 2009; Sudvery 2008; Schuster et al. 2016; Takeshita 2016; Riquelme et al. 2018; Zhou et al. 2018). Vesicle trafficking supplies the required proteins and lipids via actin, as well as microtubule cytoskeletons and their corresponding motor proteins (Fig. 1b) (Taheri-Talesh et al. 2008; Steinberg 2011; Egan et al. 2012; Penalva et al. 2017; Renshaw et al. 2016). Microtubules serve as tracks of secretory vesicles for long-distance transport to hyphal tips and are important for rapid hyphal growth (Horio and Oakley 2005; Seiler et al. 1997). Actin cables formed from the hyphal tip in the retrograde direction are involved in exocytosis and secretory vesicle accumulation before exocytosis (Berepiki et al. 2011; Bergs et al. 2016). These vesicles accumulate at the apices prior to fusion with the membrane. They form a structure called Spitzenkörper (Harris 2009), which is thought to act as a vesicle supply center, a site where cargo for the hyphal tip is sorted (Riquelme and Sánchez-León 2014).

Besides their role as tracks for vesicle traffic, microtubules are necessary to maintain the direction of hyphal growth (Riquelme et al. 1998). Polar organization of the actin cytoskeleton is mediated mainly by microtubule-dependent positioning of polarity marker proteins (Fig. 1c). One polarity marker in *Aspergillus nidulans* (TeaA) is specifically delivered to the apex by growing microtubules, and it is anchored to the apical membrane by direct interaction with another polarity marker

(TeaR) at the plasma membrane (Fig. 1c) (Fischer et al. 2008; Takeshita et al. 2008). Their interdependent interaction at the apical membrane initiates the recruitment of additional components including the formin which polymerizes actin cables for targeted cargo delivery (Higashitsuji et al. 2009). Defective polarity markers result in hyphae that are curved or zigzagged instead of straight (Takeshita et al. 2008).

In *A. nidulans*, microtubules extend all the way to the hyphal tip, whereas actin cables are found mostly near the hyphal tip (Bergs et al. 2016). Vesicles containing components of the growth machinery are transported along microtubules from posterior sites to the apical region, transferred to actin cables, and finally delivered to the apical cortex of the hypha (Egan et al. 2012; Fischer et al. 2008; Pantazopoulou et al. 2014; Taheri-Talesh et al. 2008; Takeshita et al. 2014). These secretory vesicles (SVs) are released from the trans-Golgi network after maturation (Pantazopoulou et al. 2014; Pinar et al. 2015). Since gene deletion of kinesin-1 or myosin-5 decreases the amount of SVs at the hyphal tips, resulting in growth retardation, SVs are believed to be transported along microtubules by kinesin-1 and further along actin filaments by myosin-5 to the hyphal tip for exocytosis (Pantazopoulou et al. 2014; Seiler et al. 1997; Taheri-Talesh et al. 2012). However, localization analysis reported that kinesin-1 diffuses in the cytoplasm and myosin-5 accumulates at the hyphal tip (Requena et al. 2001; Taheri-Talesh et al. 2012). SV transport was not directly observed, probably due to the small size and fast motion. Early endosomes (EEs) are easier to track, so their bi-directional transport along microtubules by kinesin-3 and dynein has been thoroughly studied (Abenza et al. 2009, 2010; Egan et al. 2012; Lenz et al. 2006; Schuster et al. 2011).

Chitin synthases are thought to be transported on SVs to the plasma membrane for new cell wall synthesis (Fig. 1d), where they are subsequently internalized by endocytosis and transported on EEs for degradation in vacuoles, or recycled back to the plasma membrane (Sacristan et al. 2012). Actin patches are peripheral punctate structures, where the endocytic machinery is probably located (Araujo-Bazán et al. 2008). Kinesin-1 is required for transport of ChsB to the subapical region. However, mechanistic details could not be resolved due to high background fluorescence near the hyphal tip, insufficient time resolution to resolve fast motions, and the inability to distinguish between SVs and EEs (Takeshita et al. 2015).

An essential role for chitin synthase phosphorylation in the polarized biosynthesis of fungal cell walls is demonstrated in the polymorphic human pathogen *Candida albicans* (Lenardon et al. 2010a, b). Class III chitin synthase (Chs3) is localized at the tips of growing buds and hyphae, and at the septum. A phospho-proteome analysis of *C. albicans* revealed that Chs3 is phosphorylated. Mutation of this site showed the phosphorylation is required for the correct localization and function of Chs3.

4 Super-resolution Imaging and Cluster Analysis of Chitin Synthase

ChsB localizes to hyphal tips and concentrates at the Spitzenkörper in *A. nidulans* (Fukuda et al. 2009). In recent study, super-resolution localization imaging and high-speed pulse-chase imaging as a powerful biophysical approach have been used to analyze ChsB transport and dynamics of the Spitzenkörper (Zhou et al. 2018). The resolution of conventional light microscopy techniques is limited to around 250–300 nm due to light diffraction. Super-resolution microscopy techniques, such as STORM, PALM, etc., have overcome the diffraction limit, resulting in lateral image resolution as high as 20 nm, providing a powerful tool to investigate protein localization in high detail (Sahl and Moerner 2013).

To quantitatively analyze the spatio-temporal development of the Spitzenkörper with very high resolution, hyphae expressing ChsB was imaged as a fusion protein with mEosFPthermo (Wiedenmann et al. 2011). The thermostable monomeric green fluorescent chromophore can be permanently photoconverted to red with near-UV irradiation (Nienhaus et al. 2005, 2006). That is widely employed for fluorescence imaging, pulse-chase experiments, and super-resolution photoactivation localization microscopy (PALM) (Betzig et al. 2006; Hess et al. 2006). PALM uses photoswitchable fluorophores to achieve temporal control of the emission through conversion between fluorescent 'on/red' and 'off/green' states. When sample excitation is a sufficient low intensity, only a random sparse fluorophore subset will be in the 'on/red' state at any time, allowing these molecules to be imaged individually, precisely localized. Such strategy leads to the construction of a super-resolution image.

Single-molecular imaging-based localization microscopy revealed a pronounced fluorescent cluster of mEos-ChsB at the hyphal apex, representing the Spitzenkörper, and multiple speckles mostly near the plasma membrane (Fig. 2a) (Zhou et al. 2018). ChsB accumulation at the hyphal tip was classified by cluster analysis, where more than 10 molecules within 50 nm are defined as a cluster (Fig. 2b). Cluster images of 2.5 s time intervals were generated for a total period of 120 s with a moving window binning technique (500 frames binning with 50 frames shift) (Fig. 2c) (Ishitsuka et al. 2015). Each cluster is shown in different colors. The cluster areas and numbers of ChsB molecules within each cluster were calculated over the time course of the experiment (Fig. 2d). The green cluster of 0.1 μm^2 containing $\sim$100 molecules is visible from 7.5–60 s. It grows via fusion with the blue cluster and evolves into the pink, crescent-shaped cluster of $\sim$0.2 μm^2 containing $\sim$200 molecules, visible from 62.5–80 s. Subsequently, this cluster breaks up into two smaller ones ($\sim$0.05–0.1 μm^2, $\sim$50–100 molecules), depicted in light green and light blue. The shape change of the cluster from globular to crescent reflects the transition from vesicle accumulation prior to exocytosis to vesicle fusion with the apical plasma membrane during exocytosis.

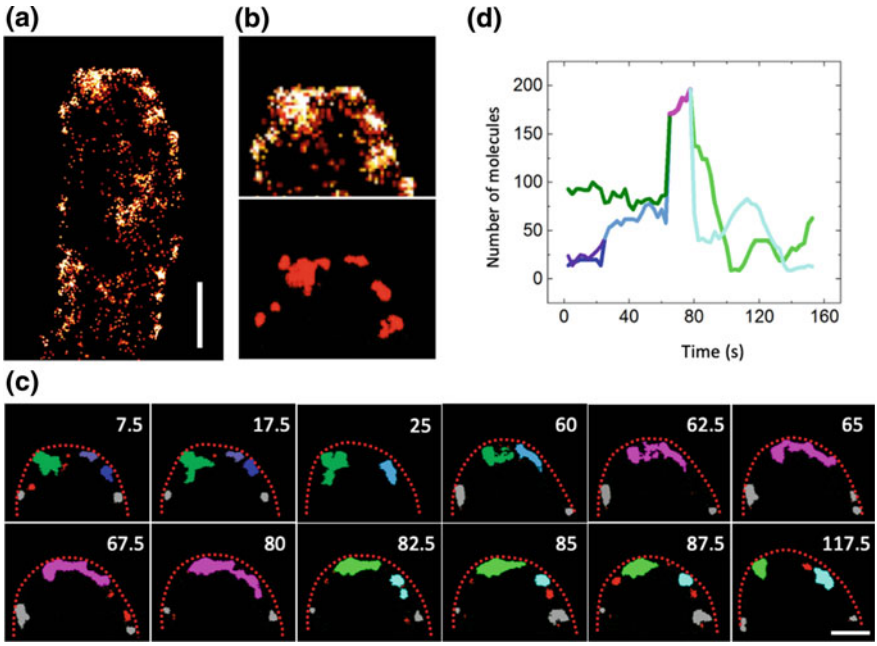

Fig. 2 Super-resolution imaging of Spitzenkörper dynamics. **a** Localization image of a hypha with mEosFP-ChsB clusters (constructed with 500 frames for 25 s). Scale bars; 1 μm. **b** Top: image of the hyphal tip. Each dot indicates single molecule. Bottom: ChsB accumulations classified by cluster analysis; more than ten molecules within 50 nm are defined as a cluster. **c** Sequence of ChsB cluster images (clusters in different colors) rendered from images reconstructed by time-lapse PALM (2.5 s interval by moving window binning for 120 s). Scale bars; 300 nm. **d** Time courses of number of ChsB molecules. Lines are drawn in colors corresponding to the clusters in (**c**) (modified Zhou et al. 2018)

5 Pulse-Chase Analysis of mEosFP-ChsB After Photoconversion

High-speed pulse-chase imaging of mEos-ChsB after photoconversion was employed to monitor its transport (Zhou et al. 2018). After photobleaching all red-emitting molecules with a 561 nm laser, a spot ~5 μm behind the hyphal tip was irradiated for 1 s with a tightly focused 405 nm laser beam to locally photoconvert mEos-ChsB to its red-emitting form (Fig. 3a). In Fig. 3b, image '0' shows the red fluorescence excited by the 405 nm laser, marking the local photoconversion spot. Then, the 561 nm laser was again switched on (image '1'), and images were acquired for 15–30 s with a dwell time of 50 ms. A large red-emitting spot appeared at the site of photoconversion, which gradually faded and dispersed due to vesicle transport away from the photoconversion region. By taking advantage of the low background in this pulse-chase imaging scheme, both anterograde (from back to tip) and retrograde (from tip to back) vesicle movements are easily observed in a kymograph along the axis of the hypha (Fig. 3c). The typical linear vesicle displacements were occasionally interrupted by brief stops, and there were also some

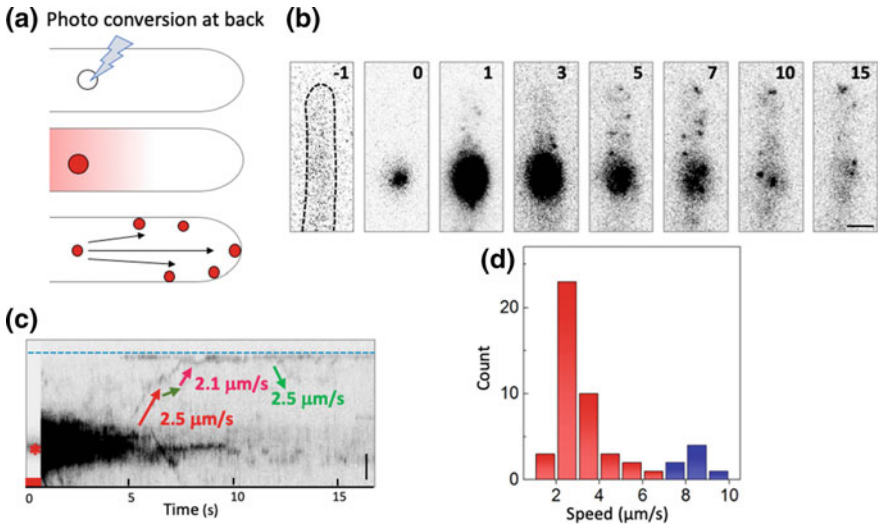

Fig. 3 High-speed pulse-chase analysis of mEos-ChsB transport. **a** Sequence of pulse-chase analysis of mEosFP-ChsB after photoconversion at back of hyphae. **b** Images of mEosFP-ChsB prior to photoconversion (−1), with 405-nm light applied at the spot marked by the dashed line for 1 s (0) and after photoconversion for 15 s. **c** Kymograph calculated from panel (**b**); arrows indicate anterograde and retrograde transport. The blue dashed line and the red asterisk mark the positions of the hyphal tip and the photoconversion locus, respectively; the red square indicates the photoconversion interval. **d** Speed distribution of anterograde transport. Slow anterograde (red) and fast anterograde (blue) transport (mean ± SD; $n = 42$, and 7, respectively) (modified Zhou et al. 2018)

immobile spots. We further noticed that the fluorescence from the hyphal tip stayed constant beyond ~5 s after photoconversion.

The slopes of the lines in the kymograph encode the speed of ChsB vesicle movement. From observations of a large number of hyphae, we noticed that most displacements occurred at speeds of 2–4 μm s^{-1}; however, there were also clearly faster processes with speeds of 7–10 μm s^{-1}. Accordingly, the speed histogram of anterograde movements appears to consist of two sub-distributions (Fig. 3d), a predominant distribution associated with slow transport centered on 3.0 ± 1.0 μm s^{-1} and a smaller distribution representing fast transport centered on 8.3 ± 0.7 μm s^{-1}. By comparison with the transport of EE and SV markers, the slow transport and fast transport were unambiguously assigned to ChsB associated with EEs and SVs, respectively. In fungi, EEs are 4–5 times larger than SVs (Gibeaux et al. 2013; Lin et al. 2016). Therefore, the slower transport of EEs is probably caused by the size of the cargo. Of note, in cultured mammalian cells, the speeds of kinesin-1 and kinesin-3 are similar, ~1–2 μm s^{-1} (Hammond et al. 2009; Tanenbaum et al. 2014). Comparative analysis using motor protein deletion mutants allowed us to assign the fast movements (7–10 μm s^{-1}) to transport of secretory vesicles by kinesin-1, and the slower ones (2–7 μm s^{-1}) to transport by kinesin-3 on early endosomes (Zhou et al. 2018). These results show how motor proteins ensure the supply of vesicles to the hyphal tip, where temporally regulated exocytosis results in stepwise tip extension.

6 Oscillation of Fungal Tip Growth

Time-lapse super-resolution PALM (photoactivation localization microscopy) analysis revealed that membrane-associated polarity marker TeaR in *A. nidulans* transiently assembles (approximately 120 nm) at the hyphal tip membrane and

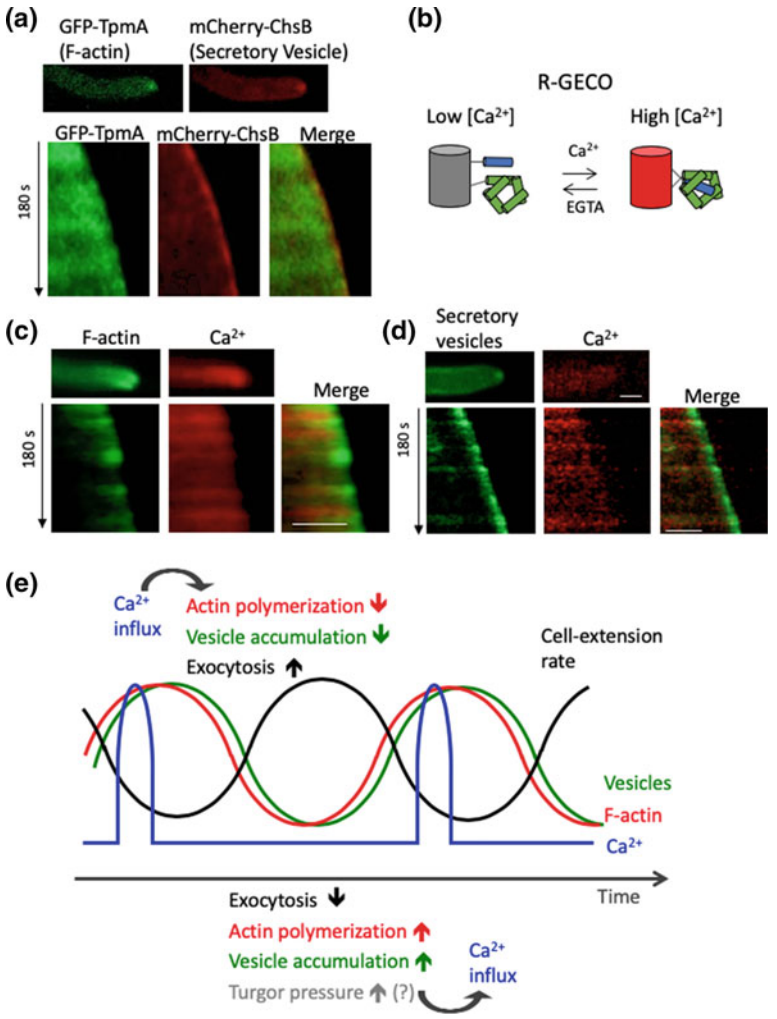

Fig. 4 Pulses of Ca^{2+} coordinate actin assembly and exocytosis. **a** Fluorescence image of F-actin and SV visualized by GFP-TpmA and mCherry-ChsB, respectively, in the growing hypha. Kymographs of F-actin (green) and SV (red) along the growth axis in the growing hypha. Total 180 s. **b** Scheme of the Ca^{2+} biosensor, R-GECO. **c**, **d** Fluorescence images and kymographs along the growth axis of F-actin (GFP-TpmA) (**c**) or secretory vesicles (GFP-BglA) (**d**) and Ca^{2+} (R-GECO). Total 180 s. Scale bar: 2 μm. (e) Scheme of oscillation in fungal tip growth coordinated by Ca^{2+} influx (modified Takeshita et al. 2017)

disperses along the membrane after exocytosis, which inserts a new membrane that results in local membrane extension (Ishitsuka et al. 2015). These findings gave rise to a 'transient polarity assembly model' to explain how fungal tip cells extend through repeated cycles of TeaR assembly/disassembly, actin polymerization, and exocytosis, rather than by constant elongation (Ishitsuka et al. 2015; Takeshita 2016). The findings of colocalization studies further support the notion that TeaR clusters represent zones of exocytosis and are prerequisite for apical membrane extension. In line with this model, recent work on *Neurospora crassa* has identified bursts of exocytotic events at various sites within the apical membrane rather than a persistent exocytosis site (Riquelme et al. 2014).

F-actin and secretory vesicles (SV) were visualized by fluorescence of GFP-tagged tropomyosin (TpmA) and mCherry-tagged ChsB, respectively (Fig. 4a) (Takeshita et al. 2017). Prominent signals were visible at the hyphal tip, and time-resolved recording and frame analysis by kymographs revealed that the signal intensity oscillated. The mean interval of the intensity of F-actin peaks was 29 ± 8 s, whereas the mean interval of peaks of SV was comparable to the one of F-actin, 30 ± 7 s. The temporal relationship between the presence of F-actin and SV was calculated as the normalized cross-correlation of their signal intensities, revealing the central peak is 0.50, indicative of a positive correlation between the signals of F-actin (green) and SV (red) (1 and −1 represent perfect positive and negative correlations, respectively). There were a few second delays in the signals of SV in comparison to the signals of F-actin, indicating that SV accumulate during actin polymerization phases and SV are depleted due to exocytosis during actin depolymerization.

7 Ca^{2+} Oscillation

Intracellular Ca^{2+} levels regulate actin assembly and vesicle fusion (Janmey 1994; Schneggenburger and Neher 2005). The red-fluorescent Ca^{2+} biosensor R-GECO was produced in *A. nidulans* (Fig. 4b) (Takeshita et al. 2017). Pulses of the R-GECO signal were observed: The mean interval between peaks was 26 ± 7 s. The R-GECO signal appeared as a tip-high gradient and diffused backwards. Such R-GECO pulses continued for multiple times before they disappeared (max. $n = 8$ in 180 s), probably due to a limited turnover of R-GECO. The fluorescence of R-GECO could not be detected in media without CaCl2 or with 1 μM CaCl2 + 10 mM EGTA, indicating that the increase of the intracellular Ca^{2+} level is induced by the influx of Ca^{2+} to the cells at hyphal tips.

The signals of R-GECO and GFP-TpmA (F-actin) or BglA-GFP (∝-glycosidase, secreted protein as a marker for SV) showed oscillation in kymographs along the growth axis indicated temporal changes of signal intensities (Fig. 4c, d). The signal intensities of F-actin (green) and the Ca^{2+} concentration (red) at the tip indicated that oscillations of peak intensities had similar periods (29 ± 8 and 26 ± 7 s, respectively) and were synchronized. Normalized cross-correlation analysis yielded

a positive correlation between the concentrations of F-actin (green) and Ca^{2+} (red), with the central peak at 0.40 and indicated that the peaks of Ca^{2+} appeared a few seconds earlier than those of F-actin. These results are in agreement with the notion that Ca^{2+} influx at the growing hypha induces actin depolymerization. Hyphae producing R-GECO and BglA-GFP (SV) also showed oscillations of the GFP intensity at the tip and R-GECO pulses (Fig. 4d), with similar periods (30 ± 7 and 26 ± 7 s, respectively), which were synchronized. Normalized cross-correlation analysis yielded a positive correlation with a central peak value of 0.43 and a few seconds delay of BglA-GFP, indicating that Ca^{2+} influx affords exocytosis mediated by fusion of SV with the plasma membrane as well as actin depolymerization.

The oscillation of Ca^{2+} levels at the hyphal tips of filamentous fungi suggested the stepwise extension of hyphal tips (Kim et al. 2012). Indeed, critical correlations were shown between intracellular Ca^{2+} levels, actin polymerization, exocytosis, and cell extension at fungal tips (Takeshita et al. 2017). Thus, the pulsed Ca^{2+} influx coordinates the temporally controlled actin polymerization and exocytosis that drive stepwise cell extension (Fig. 4e). Several Ca^{2+} channels, pumps, and transporters, such as the plasma membrane, ER, Golgi, mitochondria, and vacuoles function in fungal organelles (Zelter et al. 2004). The Ca^{2+} channels at the plasma membrane of *Saccharomyces cerevisiae*, Mid1 and Cch1p, share a single pathway that responds to environmental stressors and ensures cellular Ca^{2+} homeostasis (Iida et al. 1994; Locke et al. 2000; Paidhungat and Garrett 1997). Deletion of the orthologs *midA* and *cchA* from *A. nidulans* causes defective polarized growth and cell wall synthesis (Wang et al. 2012). Proper tip growth and the oscillation of F-actin, secretory vesicles, and growth rates require Ca^{2+} channels (Takeshita et al. 2017). The oscillatory model explains how transient Ca^{2+} influx depolymerizes F-actin at the cortex, stimulates secretory vesicles to fuse with the plasma membrane, and extends the cell tip faster. After Ca^{2+} diffusion, F-actin and secretory vesicles accumulate at hyphal tips.

The key event appears to be the activation of Ca^{2+} channels. One attractive notion is that the Ca^{2+} channels could be stretch-activated. Cells gradually build up turgor pressure against the membrane and the cell wall during slow growth phases, and Ca^{2+} channels might be activated when membrane tension exceeds a threshold. The entry of Ca^{2+} into the cell promotes exocytosis and leads to cell extension, which in turn decreases turgor pressure and inactivates the channels. Indeed, the ortholog Mid1 of *S. cerevisiae* is stretch-activated (Kanzaki et al. 1999). The next items to address would be missing links between turgor pressure and cell wall extension.

8 Biological Meaning of Oscillations

Relationships between cellular responses and receptor stimuli are encoded by the spatial and temporal dynamics of downstream signaling networks (Kholodenko 2006). Positive feedback, alone or in combination with negative feedback, can

trigger oscillations, for example, the Ca^{2+} oscillations that arise from Ca^{2+}-induced Ca^{2+} release (Goldbeter 2002). The shape of oscillations is characterized by their amplitude and phase. The frequency modulation of Ca^{2+} oscillations provides an efficient means to differentiate intracellular biological responses (Smedler and Uhlen 2014).

The oscillation of cortical F-actin presumably follows that of Ca^{2+} and correlates with the oscillations of vesicle secretion. These coordinated steps result in growth oscillation (Takeshita 2018). A feedback cycle might be efficient for all these steps to continuously proceed. In addition, oscillatory cell growth allows cells to respond more rapidly and frequently to internal and external cues such as chemical or mechanical environmental signals. Indeed, Ca^{2+} influx by Ca^{2+} channels is involved in the control of directional hyphal growth in *C. albicans* (Brand et al. 2007). The influx of Ca^{2+} promotes Cdc42 GTPase trafficking and amplifies Cdc42-mediated directional growth signals (Brand et al. 2014). Stepwise growth coordinated by a transient Ca^{2+} influx might link growth with chemotropism and chemotaxis. Cell–cell fusion is essential for colony development in *N. crassa* (Herzog et al. 2015). Before growing partners fuse in a tip-to-tip manner, the cells coordinately switch between two physiological stages via the oscillatory recruitment of a MAP kinase (MAK-2) and a protein of unknown molecular function (SO) to the apical plasma membrane of growing fusion tips (Fleissner et al. 2009; Serrano et al. 2017). The oscillation of signaling, which is probably related to signal sending and signal receiving, allows cells to coordinate their behavior and achieve efficient cell fusion (Goryachev et al. 2012).

9 Conclusion and Perspective

The dynamic responses to external and internal signals are fundamental to the increased understanding of chemotropism, cell–cell fusion, microbial interaction, and the fungal penetration of plant and animal cells. The pulsed Ca^{2+} influx coordinates the temporally controlled actin polymerization and exocytosis that drive stepwise cell extension of filamentous fungi. Besides them, to understand the hyphal tip growth, we need to pay attention to the balance between turgor pressure and cell wall pressure, which is regulated by cell wall synthesis, degradation, and maturation. The filamentous fungus elongates hyphae by tip growth while forming a cell wall comprising a complex three-dimensional structure. Understanding the cell wall biosynthesis is very important in understanding the interaction with other microorganisms and the infection mechanism of filamentous fungi to plants and animals. Recent studies have identified many glycosyltransferase genes involved in biosynthesis of constituent polysaccharides. Next open questions are the formation mechanism of the polysaccharide structure which changes according to the environmental changes and the cell wall formation mechanism at the time of differentiation, also how all the chitin and glucan synthases and cell wall relating proteins are trafficking coordinated in the formation of the cell wall skeletons.

References

Abenza JF, Galindo A, Pantazopoulou A, Gil C, de los Rios V, Penalva MA (2010) *Aspergillus* RabB Rab5 integrates acquisition of degradative identity with the long distance movement of early endosomes. Mol Biol Cell 21:2756–69

Abenza JF, Pantazopoulou A, Rodriguez JM, Galindo A, Penalva MA (2009) Long-distance movement of *Aspergillus nidulans* early endosomes on microtubule tracks. Traffic 10:57–75

Araujo-Bazan L, Penalva MA, Espeso EA (2008) Preferential localization of the endocytic internalization machinery to hyphal tips underlies polarization of the actin cytoskeleton in *Aspergillus nidulans*. Mol Microbiol 67:891–905

Berepiki A, Lichius A, Read ND (2011) Actin organization and dynamics in filamentous fungi. Nat Rev Microbiol 9:876–887

Bergs A, Ishitsuka Y, Evangelinos M, Nienhaus GU, Takeshita N (2016) Dynamics of actin cables in polarized growth of the filamentous fungus *Aspergillus nidulans*. Front Microbiol 7:682

Betzig E, Patterson GH, Sougrat R, Lindwasser OW, Olenych S et al (2006) Imaging intracellular fluorescent proteins at nanometer resolution. Science 313:1642–1645

Blumenthal HJ, Roseman S (1957) Quantitative estimation of chitin in fungi. J Bacteriol 74:222–224

Borgia PT, Iartchouk N, Riggle PJ, Winter KR, Koltin Y, Bulawa CE (1996) The *chsB* gene of *Aspergillus nidulans* is necessary for normal hyphal growth and development. Fungal Genet Biol 20:193–203

Brand A, Shanks S, Duncan VM, Yang M, Mackenzie K, Gow NA (2007) Hyphal orientation of *Candida albicans* is regulated by a calcium-dependent mechanism. Curr Biol 17:347–352

Brand AC, Morrison E, Milne S, Gonia S, Gale CA, Gow NA (2014) Cdc42 GTPase dynamics control directional growth responses. Proc Natl Acad Sci USA 111:811–816

de Groot PW, Brandt BW, Horiuchi H, Ram AF, de Koster CG, Klis FM (2009) Comprehensive genomic analysis of cell wall genes in *Aspergillus nidulans*. Fungal Genet Biol 46:S72–S81

Egan MJ, Tan K, Reck-Peterson SL (2012) Lis1 is an initiation factor for dynein-driven organelle transport. J Cell Biol 197:971–982

Fischer R, Zekert N, Takeshita N (2008) Polarized growth in fungi—interplay between the cytoskeleton, positional markers and membrane domains. Mol Microbiol 68:813–826

Fleissner A, Leeder AC, Roca MG, Read ND, Glass NL (2009) Oscillatory recruitment of signaling proteins to cell tips promotes coordinated behavior during cell fusion. Proc Natl Acad Sci USA 106:19387–19392

Fukuda K, Yamada K, Deoka K, Yamashita S, Ohta A, Horiuchi H (2009) Class III chitin synthase ChsB of *Aspergillus nidulans* localizes at the sites of polarized cell wall synthesis and is required for conidial development. Eukaryot Cell 8:945–956

Fujiwara M, Horiuchi H, Ohta A, Takagi M (1997) A novel fungal gene encoding chitin synthase with a myosin motor-like domain. Biochem Biophys Res Commun 236:75–78

Fujiwara M, Ichinomiya M, Motoyama T, Horiuchi H, Ohta A, Takagi M (2000) Evidence that the *Aspergillus nidulans* class I and class II chitin synthase genes, *chsC* and *chsA*, share critical roles in hyphal wall integrity and conidiophore development. J Biochem 127:359–366

Gibeaux R, Hoepfner D, Schlatter I, Antony C, Philippsen P (2013) Organization of organelles within hyphae of *Ashbya gossypii* revealed by electron tomography. Eukaryot Cell 12:1423–1432

Goldbeter A (2002) Computational approaches to cellular rhythms. Nature 420:238–245

Gonçalves I, Brouillet S, Soulie MC, Gribaldo S, Sirven C, Charron N, Boccara M, Choquer M (2016) Genome-wide analyses of chitin synthases identify horizontal gene transfers towards bacteria and allow a robust and unifying classification into fungi. BMC Evol Biol 16:252

Goryachev AB, Lichius A, Wright GD, Read ND (2012) Excitable behavior can explain the "ping-pong" mode of communication between cells using the same chemoattractant. BioEssays 34:259–266

Hammond JW, Cai D, Blasius TL, Li Z, Jiang Y et al (2009) Mammalian Kinesin-3 motors are dimeric in vivo and move by processive motility upon release of autoinhibition. PLoS Biol 7: e72

Harris SD (2009) The Spitzenkörper: a signalling hub for the control of fungal development? Mol Microbiol 73:733–736

Herzog S, Schumann MR, Fleissner A (2015) Cell fusion in *Neurospora crassa*. Curr Opin Microbiol 28:53–59

Hess ST, Girirajan TP, Mason MD (2006) Ultra-high resolution imaging by fluorescence photoactivation localization microscopy. Biophys J 91:4258–4272

Higashitsuji Y, Herrero S, Takeshita N, Fischer R (2009) The cell end marker protein TeaC is involved in growth directionality and septation in *Aspergillus nidulans*. Eukaryot Cell 8:957–967

Horio T, Oakley BR (2005) The role of microtubules in rapid hyphal tip growth of *Aspergillus nidulans*. Mol Biol Cell 16:918–926

Horiuchi H (2009) Functional diversity of chitin synthases of *Aspergillus nidulans* in hyphal growth, conidiophore development and septum formation. Med Mycol 47(Suppl 1):S47–S52

Ichinomiya M, Yamada E, Yamashita S, Ohta A, Horiuchi H (2005) Class I and class II chitin synthases are involved in septum formation in the filamentous fungus *Aspergillus nidulans*. Eukaryot Cell 4:1125–1136

Iida H, Nakamura H, Ono T, Okumura MS, Anraku Y (1994) MID1, a novel *Saccharomyces cerevisiae* gene encoding a plasma membrane protein, is required for Ca^{2+} influx and mating. Mol Cell Biol 14:8259–8271

Ishitsuka Y, Savage N, Li Y, Bergs A, Grun N, Kohler D, Donnelly R, Nienhaus GU, Fischer R, Takeshita N (2015) Superresolution microscopy reveals a dynamic picture of cell polarity maintenance during directional growth. Sci Adv 1:e1500947

Janmey PA (1994) Phosphoinositides and calcium as regulators of cellular actin assembly and disassembly. Annu Rev Physiol 56:169–191

Johnston IR (1965) The composition of the cell wall of *Aspergillus niger*. Biochem J 96:651–658

Kanzaki M, Nagasawa M, Kojima I, Sato C, Naruse K et al (1999) Molecular identification of a eukaryotic, stretch-activated nonselective cation channel. Science 285:882–886

Kholodenko BN (2006) Cell-signalling dynamics in time and space. Nat Rev Mol Cell Biol 7:165–176

Kim HS, Czymmek KJ, Patel A, Modla S, Nohe A et al (2012) Expression of the Cameleon calcium biosensor in fungi reveals distinct Ca(2+) signatures associated with polarized growth, development, and pathogenesis. Fungal Geneti Biol 49:589–601

Kobayashi T, Abe K, Asai K, Gomi K, Juvvadi PR et al (2007) Genomics of *Aspergillus oryzae*. Biosci Biotechnol Biochem 71:646–670

Latgé JP, Beauvais A, Chamilos G (2017) The cell wall of the human fungal pathogen *Aspergillus fumigatus*: biosynthesis, organization, immune response, and virulence. Annu Rev Microbiol 71:99–116

Lenardon MD, Munro CA, Gow NAR (2010a) Chitin synthesis and fungal pathogenesis. Curr Opin Microbiol 13:416–423

Lenardon MD, Milne SA, Mora-Montes HM, Kaffarnik FA, Peck SC, Brown AJ, Munro CA, Gow NA (2010b) Phosphorylation regulates polarisation of chitin synthesis in *Candida albicans*. J Cell Sci 123:2199–2206

Lenz JH, Schuchardt I, Straube A, Steinberg G (2006) A dynein loading zone for retrograde endosome motility at microtubule plus-ends. EMBO J 25:2275–2286

Lin C, Schuster M, Guimaraes SC, Ashwin P, Schrader M et al (2016) Active diffusion and microtubule-based transport oppose myosin forces to position organelles in cells. Nat Commun 7:11814

Locke EG, Bonilla M, Liang L, Takita Y, Cunningham KW (2000) A homolog of voltage-gated Ca(2+) channels stimulated by depletion of secretory Ca(2+) in yeast. Mol Cell Biol 20:6686–6694

Lopez-Franco R, Bartnicki-Garcia S, Bracker CE (1994) Pulsed growth of fungal hyphal tips. Proc Natl Acad Sci USA 91:12228–12232

Motoyama T, Kojima N, Horiuchi H, Ohta A, Takagi M (1994) Isolation of a chitin synthase gene (*chsC*) of *Aspergillus nidulans*. Biosci Biotechnol Biochem 58:2254–2257

Muszkieta L, Aimanianda V, Mellado E, Gribaldo S, Alcàzar-Fuoli L, Szewczyk E, Prevost MC, Latgé JP (2014) Deciphering the role of the chitin synthase families 1 and 2 in the in vivo and in vitro growth of *Aspergillus fumigatus* by multiple gene targeting deletion. Cell Microbiol 16:1784–1805

Nienhaus GU, Nienhaus K, Holzle A, Ivanchenko S, Renzi F et al (2006) Photoconvertible fluorescent protein EosFP: biophysical properties and cell biology applications. Photochem Photobiol 82:351–358

Nienhaus K, Nienhaus GU, Wiedenmann J, Nar H (2005) Structural basis for photo-induced protein cleavage and green-to-red conversion of fluorescent protein EosFP. Proc Natl Acad Sci USA 102:9156–9159

Paidhungat M, Garrett S (1997) A homolog of mammalian, voltage-gated calcium channels mediates yeast pheromone-stimulated Ca^{2+} uptake and exacerbates the cdc1(Ts) growth defect. Mol Cell Biol 17:6339–6347

Pantazopoulou A, Pinar M, Xiang X, Penalva MA (2014) Maturation of late Golgi cisternae into RabE(RAB11) exocytic post-Golgi carriers visualized in vivo. Mol Biol Cell 25:2428–2443

Penalva MA, Zhang J, Xiang X, Pantazopoulou A (2017) Transport of fungal RAB11 secretory vesicles involves myosin-5, dynein/dynactin/p25 and kinesin-1 and is independent of kinesin-3. Mol Biol Cell 28:947–961

Perez-Nadales E, Nogueira MF, Baldin C, Castanheira S, El Ghalid M et al (2014) Fungal model systems and the elucidation of pathogenicity determinants. Fungal Genet Biol 70:42–67

Pinar M, Arst HN, Jr., Pantazopoulou A, Tagua VG, de los Rios V et al (2015) TRAPPII regulates exocytic Golgi exit by mediating nucleotide exchange on the Ypt31 ortholog RabERAB11. Proc Natl Acad Sci USA 112:4346–51

Punt PJ, van Biezen N, Conesa A, Albers A, Mangnus J, van den Hondel C (2002) Filamentous fungi as cell factories for heterologous protein production. Trends Biotechnol 20:200–206

Riquelme M, Aguirre J, Bartnicki-García S, Braus GH, Feldbrügge M, Fleig U, Hansberg W, Herrera-Estrella A, Kämper J, Kück U, Mouriño-Pérez RR, Takeshita N, Fischer R (2018) Fungal morphogenesis, from the polarized growth of hyphae to complex reproduction and infection structures. Microbiol Mol Biol Rev 82:e00068–17

Renshaw H, Vargas-Muñiz JM, Richards AD, Asfaw YG, Juvvadi PR, Steinbach WJ (2016) Distinct roles of myosins in *Aspergillus fumigatus* hyphal growth and pathogenesis. Infect Immun 84:1556–1564

Requena N, Alberti-Segui C, Winzenburg E, Horn C, Schliwa M et al (2001) Genetic evidence for a microtubule-destabilizing effect of conventional kinesin and analysis of its consequences for the control of nuclear distribution in *Aspergillus nidulans*. Mol Microbiol 42:121–132

Riquelme M, Bredeweg EL, Callejas-Negrete O, Roberson RW, Ludwig S et al (2014) The *Neurospora crassa* exocyst complex tethers Spitzenkörper vesicles to the apical plasma membrane during polarized growth. Mol Biol Cell 25:1312–1326

Riquelme M, Reynaga-Pena CG, Gierz G, Bartnicki-Garcia S (1998) What determines growth direction in fungal hyphae? Fungal gGenet Biol 24:101–109

Riquelme M, Sanchez-Leon E (2014) The Spitzenkörper: a choreographer of fungal growth and morphogenesis. Curr Opin Microbiol 20:27–33

Riquelme M, Yarden O, Bartnicki-Garcia S, Bowman B, Castro-Longoria E et al (2011) Architecture and development of the *Neurospora crassa* hypha—a model cell for polarized growth. Fungal Biol 115:446–474

Rittenour WR, Si H, Harris SD (2009) Hyphal morphogenesis in *Aspergillus nidulans*. Fungal Biol Rev 23:20–29

Rogg LE, Fortwendel JR, Juvvadi PR, Steinbach WJ (2012) Regulation of expression, activity and localization of fungal chitin synthases. Med Mycol 50:2–17

Sacristan C, Reyes A, Roncero C (2012) Neck compartmentalization as the molecular basis for the different endocytic behaviour of Chs3 during budding or hyperpolarized growth in yeast cells. Mol Microbiol 83:1124–1135

Sahl SJ, Moerner WE (2013) Super-resolution fluorescence imaging with single molecules. Curr Opin Struct Biol 23:778–787

Schneggenburger R, Neher E (2005) Presynaptic calcium and control of vesicle fusion. Curr Opin Neurobiol 15:266–274

Schuster M, Kilaru S, Fink G, Collemare J, Roger Y, Steinberg G (2011) Kinesin-3 and dynein cooperate in long-range retrograde endosome motility along a nonuniform microtubule array. Mol Biol Cell 22:3645–3657

Schuster M, Martin-Urdiroz M, Higuchi Y, Hacker C, Kilaru S, Gurr SJ, Steinberg G (2016) Co-delivery of cell-wall-forming enzymes in the same vesicle for coordinated fungal cell wall formation. Nat Microbiol 1:16149

Seiler S, Nargang FE, Steinberg G, Schliwa M (1997) Kinesin is essential for cell morphogenesis and polarized secretion in *Neurospora crassa*. EMBO J 16:3025–3034

Serrano A, Hammadeh HH, Herzog S, Illgen J, Schumann MR et al (2017) The dynamics of signal complex formation mediating germling fusion in *Neurospora crassa*. Fungal Genet Biol 101:31–33

Smedler E, Uhlen P (2014) Frequency decoding of calcium oscillations. Biochim Biophys Acta 1840:964–969

Steinberg G (2011) Motors in fungal morphogenesis: cooperation versus competition. Current Opin Microbiol 14:660–667

Sudvery PE (2008) Regulation of polarized growth in fungi. Fungal Biol Rev 22:44–55

Taheri-Talesh N, Horio T, Araujo-Bazan L, Dou X, Espeso EA et al (2008) The tip growth apparatus of *Aspergillus nidulans*. Mol Biol Cell 19:1439–1449

Taheri-Talesh N, Xiong Y, Oakley BR (2012) the Functions of myosin II and myosin V homologs in tip growth and septation in *Aspergillus nidulans*. PLoS ONE 7:e31218

Takeshita N (2016) Coordinated process of polarized growth in filamentous fungi. Biosci Biotech Biochem 80:1693–1699

Takeshita N (2018) Oscillatory fungal cell growth. Fungal Genet Biol 110:10–14

Takeshita N, Evangelinos M, Zhou L, Serizawa T, Somera-Fajardo RA et al (2017) Pulses of Ca^{2+} coordinate actin assembly and exocytosis for stepwise cell extension. Proc Natl Acad Sci USA 114:5701–5706

Takeshita N, Higashitsuji Y, Konzack S, Fischer R (2008) Apical sterol-rich membranes are essential for localizing cell end markers that determine growth directionality in the filamentous fungus *Aspergillus nidulans*. Mol Biol Cell 19:339–351

Takeshita N, Manck R, Grun N, de Vega SH, Fischer R (2014) Interdependence of the actin and the microtubule cytoskeleton during fungal growth. Curr Opin Microbiol 20:34–41

Takeshita N, Ohta A, Horiuchi H (2005) CsmA, a class V chitin synthase with a myosin motor-like domain, is localized through direct interaction with the actin cytoskeleton in *Aspergillus nidulans*. Mol Biol Cell 16:1961–1970

Takeshita N, Yamashita S, Ohta A, Horiuchi H (2006) *Aspergillus nidulans* class V and VI chitin synthases CsmA and CsmB, each with a myosin motor-like domain, perform compensatory functions that are essential for hyphal tip growth. Mol Microbiol 59:1380–1394

Takeshita N, Wernet V, Tsuizaki M, Grun N, Hoshi HO et al (2015) Transportation of *Aspergillus nidulans* class III and V chitin synthases to the hyphal tips depends on conventional kinesin. PLoS ONE 10:e0125937

Tanenbaum ME, Gilbert LA, Qi LS, Weissman JS, Vale RD (2014) A protein-tagging system for signal amplification in gene expression and fluorescence imaging. Cell 159:635–646

Wang S, Cao J, Liu X, Hu H, Shi J et al (2012) Putative calcium channels CchA and MidA play the important roles in conidiation, hyphal polarity and cell wall components in *Aspergillus nidulans*. PLoS ONE 7:e46564

Wiedenmann J, Gayda S, Adam V, Oswald F, Nienhaus K et al (2011) From EosFP to mIrisFP: structure-based development of advanced photoactivatable marker proteins of the GFP-family. J Biophotn 4:377–390

Yanai K, Kojima N, Takaya N, Horiuchi H, Ohta A, Takagi M (1994) Isolation and characterization of two chitin synthase genes from *Aspergillus nidulans*. Biosci Biotechnol Biochem 58:1828–1835

Zelter A, Bencina M, Bowman BJ, Yarden O, Read ND (2004) A comparative genomic analysis of the calcium signaling machinery in *Neurospora crassa, Magnaporthe grisea*, and *Saccharomyces cerevisiae*. Fungal Genet Biol 41:827–841

Zhou L, Evangelinos M, Wernet V, Eckert AF, Ishitsuka Y, Fischer R, Nienhaus GU, Takeshita N (2018) Superresolution and pulse-chase imaging reveal the role of vesicle transport in polar growth of fungal cells. Sci Adv 4:e1701798